Analytical and Bioanalytical Chemistry
https://doi.org/10.1007/s00216-020-02887-z

RESEARCH PAPER

A label-free lead(II) ion sensor based on surface plasmon resonance and DNAzyme-gold nanoparticle conjugates

Huanan Wu[1] · Shuokang Wang[1] · Sam Fong Yau Li[2] · Qi Bao[1] · Qiyong Xu[1]

Received: 25 May 2020 / Revised: 6 August 2020 / Accepted: 14 August 2020

Abstract

Detection of lead(II) (Pb^{2+}) ions in water is important for the protection of human health and environment. The growing demand for onsite detection still faces challenges for sensitive and easy-to-use methods. In this work, a novel surface plasmon resonance (SPR) biosensor based on GR-5 DNAzyme and gold nanoparticles (AuNPs) was developed. Thiolated DNAzyme was immobilized on the gold surface of the sensor chip followed by anchoring the substrate-functionalized AuNPs through the DNAzyme-substrate hybridization. The coupling between the localized surface plasmon (LSP) of AuNPs and the surface plasmon polaritons (SPP) on the gold sensor surface was used to improve the sensitivity. The substrate cleavage in the presence of Pb^{2+} ions was catalyzed by DNAzyme, leading to the removal of AuNPs and the diminished LSP-SPP coupling. The optimal detection limit was 80 pM for the sensor fabricated with 1 μM DNAzyme, corresponding to two or three orders of magnitude lower than the toxicity levels of Pb^{2+} in drinking water defined by WHO and USEPA. By tuning the surface coverage of DNAzyme, the sensitivity and dynamic range could be controlled. This sensor also featured high selectivity to Pb^{2+} ions and simple detection procedure. Successful detection of Pb^{2+} ions in groundwater indicates that this method has the prospect in the onsite detection of Pb^{2+} ions in water. Given the variety of AuNPs and metal-specific DNAzymes, this detection strategy would lead to the development of more sensitive and versatile heavy metal sensors.

Keywords DNAzyme · Surface plasmon resonance · Gold nanoparticles · Lead(II) ions

Introduction

Lead(II) (Pb^{2+}) ions are highly toxic heavy metal ions widely distributed in industrial wastewater, and they are hazardous to human health and environment through water contamination [1]. The maximum concentrations of lead in drinking water set by the World Health Organization (WHO) and the United States Environmental Protection Agency (EPA) are 48 nM and 72 nM, respectively [2]. Detection and analysis of lead ions are in growing demands, but they are mostly done with sophisticated instruments in laboratories, such as the inductively coupled plasma (ICP) technique integrated with optical emission spectrometer (ICP-OES), atomic emission spectroscopy (ICP-AES) and mass spectrometry (ICP-MS) [3, 4], and spectroscopic methods including atomic absorption spectroscopy (AAS) [5] and atomic fluorescence spectrometry (AFS) [6], as well as anodic stripping voltammetry (ASV) [7]. Although these conventional laboratory methods can provide very low detection limits and high accuracy, most of these methods rely on expensive equipment and relatively complicated sample preparation processes. Meanwhile, these methods require professionally trained instrument operators and cannot be used for onsite detection [8]. Therefore, the current research focuses more on the development of methods for rapid detection of Pb^{2+} ions that is portable, cost-effective, and easy to use [9, 10]. Biosensors employing biological recognition elements have emerged as a promising category of techniques in the last few decades [11].

DNAzyme-based biosensors have been potently investigated for the detection of Pb^{2+} ions [12]. DNAzyme is a single-

Electronic supplementary material The online version of this article (https://doi.org/10.1007/s00216-020-02887-z) contains supplementary material, which is available to authorized users.

✉ Qiyong Xu
qiyongxu@pkusz.edu.cn

[1] Shenzhen Engineering Laboratory for Eco-Efficient Recycled Materials, School of Environment and Energy, Peking University Shenzhen Graduate School, Shenzhen 518055, Guangdong, China

[2] Department of Chemistry, National University of Singapore, Singapore 117543, Singapore

Published online: 23 August 2020

strand DNA with the catalytic activity on specific metal ion-DNA interactions. It features low synthesis cost and high stability against denaturing, repeated refolding, and thermal conditions [13–15]. Its high specificity relies on its high catalytic activity only when specific metal ions are present [16, 17]. For example, the specificity of the GR-5 DNAzyme for Pb^{2+} is 40,000 times higher than that of other competing metal ions [18], and DNAzyme with even higher specificities keeps emerging [19, 20]. Various Pb^{2+} ion sensors using DNAzyme as a recognition element have been established based on fluorescence [21–23], colorimetry [24], electrochemistry [25–27], and surface-enhanced Raman scattering (SERS) [28, 29]. However, some of these methods suffer from using contaminating reagents, false fluorescent quenching, or tedious detection procedure. In order to solve these problems, dissipative quartz crystal microbalance (QCM-D) with a simple and sensitive DNAzyme-functionalized sensor chip has been developed [30].

The surface plasmon resonance (SPR) sensor is another type of sensor widely used for the detection of metal ions [31]. In a typical SPR metal ion sensor system, the angle or spectral characteristics of the light reflected by the prism/sensor chip interface convey information about the interactions between molecules involving the recognition element and metal ions. Compared with other sensors, SPR has the advantages of simple sample preparation and label-free, direct analysis in real time, which enables rapid detection and onsite applications [32]. More importantly, the SPR sensor can be miniaturized into low-cost chips [33] and even integrated with a smart phone for economical and efficient portable detection [34]. At present, the research of SPR sensors is mainly focused on selecting and designing a recognition element to improve the selectivity and sensitivity of target detection [35].

Gold nanoparticles (AuNPs) demonstrate a special presence of SPR due to the localized surface plasmon (LSP). Since Natan's group reported that AuNPs significantly enhanced the sensitivity of SPR sensors [36], electromagnetic interactions between AuNPs and SPR sensor chips have been widely used to improve the sensitivity of biosensors [37, 38]. Wang and co-workers have reported that AuNPs lowered the mercury ion detection limit by two orders of magnitude [39]. In addition to the extra mass and refractive index introduced to the sensor surface by AuNPs, electronic coupling interaction between the LSP of AuNPs and the surface plasmon polaritons (SPP) of the gold sensor chip (LSP-SPP coupling) has contributed to the signal amplification [40]. This AuNP-induced plasmonic amplification is unique for SPR sensors compared with other sensors such as electrochemical and QCM-D sensors. However, a DNAzyme-based SPR sensor for Pb^{2+} detection with AuNP amplification has not been reported.

To cope with the growing demand for detection of Pb^{2+} ions in water, it is important to design an easy-to-use detection method with high sensitivity. In this work, we report an SPR sensor based on GR-5 DNAzyme as a recognition element and AuNPs as a signal amplifier for ultrasensitive and selective detection of Pb^{2+}. The surface coverages of DNAzyme and AuNPs are characterized and optimized to determine their effects on sensor performance. The signal amplification due to LSP-SPP coupling is proposed. The feasibility of this sensor for the field samples of groundwater is also tested. This label-free detection strategy would benefit rapid heavy metal detection, especially when onsite measurements are desired.

Experimental

Materials

The oligonucleotides used in the present study were synthesized and HPLC-purified by Shanghai Sangon Biotechnology Co., Ltd. (Shanghai, China). The DNAzyme and substrate sequences were 5′-HS-$(CH_2)_6$-TTTACATCATCTCT GAAGTAGCGCCGCCGTATAGTGA-3′ and 5′-HS-$(CH_2)_6$-TTTTTTTTTTTTTCACTATrAGGAAGAG ATGATGT-3′, respectively. In order to facilitate the LSP-SPP coupling, the DNAzyme sequence had a shorter thymine-rich spacer sequence compared with the literature [30]. HEPES, phosphate buffer solution (PBS) containing KH_2PO_4 and Na_2HPO_4 (0.05 M, pH = 7.4), tris(2-carboxyethyl) phosphine (TCEP), 6-mer-captohexanol (MCH), and all metal salts were purchased from Aladdin (Shanghai, China). AuNPs were purchased from Abace Biology (Beijing, China). All chemicals were of analytical-reagent grade. Ultrapure water with a resistivity of 18.2 MΩ cm (Millipore) was used in the experiments.

Preparation of substrate-functionalized gold nanoparticles

Substrate-functionalized gold nanoparticles (S-AuNPs) were prepared according to literature with some modifications [30]. TCEP was added to the substrate solution and reacted at room temperature for 1 h to reduce disulfide bonds. The treated substrate solution (100 μL, 36 μM) was added to 900 μL AuNP solution, incubated at 4 °C for 16 h followed by the addition of NaCl (0.5 M, 300 μL) and PBS (250 μL). After aging at 4 °C for 40 h, the S-AuNP conjugate was centrifuged at 13,000 rpm for 30 min followed by removing the supernatant and re-dispersing the red precipitate into a working buffer solution containing 25 mM HEPES solution and 100 mM NaCl (pH = 7.4). This washing process was repeated three times for the unbound substrate to be thoroughly washed away before being stored at 4 °C. The UV-visible absorption spectra of AuNPs before and after the functionalization with the substrate were scanned using a Shimadzu 2600 spectrometer.

Sensor fabrication

The SPR102-AU sensor chips (45-nm gold-coated glass slides, BioNavis, Tampere, Finland) were cleaned with a solution containing ammonia and hydrogen peroxide (1:1:5 30% ammonia/30% hydrogen peroxide/water) for 10 min, rinsed thoroughly with ultrapure water, and dried with nitrogen gas. The cleaned sensor chips were incubated with the prepared thiolated DNAzyme solution in PBS for 16 h at 4 °C. The sensor chip surfaces were then passivated with 1 mM MCH for 60 min. Subsequently, the DNAzyme-MCH-modified sensor chips were incubated with the prepared S-AuNP solution in an 80 °C water bath for 15 min and cooled slowly down to room temperature. The fabricated sensor chip was then incubated in a working buffer for 1 h at 37 °C to remove any physisorbed substrate strands and dried by nitrogen gas.

SPR detection of Pb^{2+}

SPR measurements were conducted on a Kretschmann-type SPR instrument (SPR Navi 200, BioNavis, Tampere, Finland) equipped with a polarized laser diode (LD) with a wavelength of 670 nm as the light source and a prism with a refraction index of 1.61. The sensor chip was consisting of a glass slide coated with a 50-nm-thick gold layer and a 5-nm titanium sublayer as the adhesive layer. The glass side of the chip was mounted to the prism/chip/flow cell assembly for easy handling, and the gold surface was in direct contact with solutions flowing in the flow cell channels. Buffer and sample solutions were injected into the testing channel of the flow cell through an injector valve and a sample loop of 1 mL. The control channel for noise referencing was not used in this study so that the noise level could be comparable with a portable SPR instrument. After equilibration with the working buffer, the sensor surface was incubated with various concentrations (10~1000 nM) of Pb^{2+} in working buffer for 25 min, after which the flow was switched back to the working buffer. The entire detection procedure was performed at 37 °C with a flow rate of 40 μL min^{-1}, and the SPR angular reflective intensity curves were recorded. The selectivity of this sensing system was also evaluated by measuring the SPR response of the system towards other common metal ions.

Characterization of sensor chips

The X-ray photoelectron spectroscopy (XPS) spectra were recorded using an ESCALAB 250Xi system (Thermo Fisher, UK) with monochromatic Al Kα X-ray radiation (1486.6 eV). The analysis zone consisted in a 900-μm-diameter spot. Survey scans (binding energy from 1100 to 0 eV) and high-resolution scans (for Au 4f, C 1s, N 1s, O 1s, S 2p, and P 2p regions) were acquired at room temperature. The binding energies were corrected with reference to the Au $4f_{7/2}$ peak at 83.9 eV. A field emission scanning electron microscope (FESEM) (Supra 55, Carl Zeiss, Germany) was used to obtain the topographic images of the sensor chips in different steps of the detection strategy. The magnification was 50K.

Results and discussion

Detection strategy of the SPR biosensor

The GR-5 DNAzyme and substrate were used for Pb^{2+} ion sensor fabrication. To improve the sensor sensitivity, substrate-functionalized AuNPs (S-AuNPs) were used to amplify the SPR signal. Spherical AuNPs were selected due to the advantage of isotropic dielectric properties and orientation-independent plasmonic signals compared with nanorod [41]. The 5′-end of the substrate was extended with a thymine-rich spacer sequence and modified with thiol groups for efficient binding to AuNPs. The UV-visible absorption peaks of AuNPs undergo a slight red shift after modification with the substrate, indicating that the substrate successfully binds to AuNPs (see Electronic Supplementary Material (ESM) Fig. S1). The schematic diagram of the detection strategy and signal amplification mechanism is shown in Fig. 1. For the sensor fabrication, the GR-5 DNAzyme was firstly immobilized on the SPR sensor chip through the strong Au-S bond between the thiol terminal of DNAzyme and the gold surface of SPR sensor chips, followed by treatment with 6-mercaptohexanol (MCH) for coverage control. Subsequently, the obtained DNAzyme monolayer was annealed with S-AuNPs for efficient hybridization. In the presence of Pb^{2+}, the cleavage of the substrate strand at the rA position leads to the removal of AuNPs from the sensor surface.

The immobilization of thiol-modified DNAzyme on the gold chip surface was characterized by XPS. XPS is an efficient technique for studying the density and coverage of thiol-modified DNA on gold surfaces. The XPS survey spectra of the bare (blank) and DNAzyme-modified sensor chips are shown in Fig. 2. In each spectrum, the most obvious peaks can be identified at a binding energy of 83.9 eV and 87.6 eV, corresponding to the Au $4f_{7/2}$ and Au $4f_{5/2}$ transitions of metallic gold, respectively. The energy splitting of 3.7 eV between the two peaks is characteristic for Au $4f_{7/2}$ and Au $4f_{5/2}$ of the same Au chemical state. The appearance of C 1s (284.5–285.0 eV), N 1s (400.0–400.5 eV), and O 1s (532.4–532.6 eV) peaks indicated the presence of DNAzymes on the gold surface. The formation of DNAzyme films on the chip surface was further verified by the high-resolution XPS spectra. Peaks observed around 161.9 and 133.7 eV are ascribed to S 2p and P 2p, respectively, as shown in Fig. S2 (see ESM). The binding energies of all these peaks are consistent with

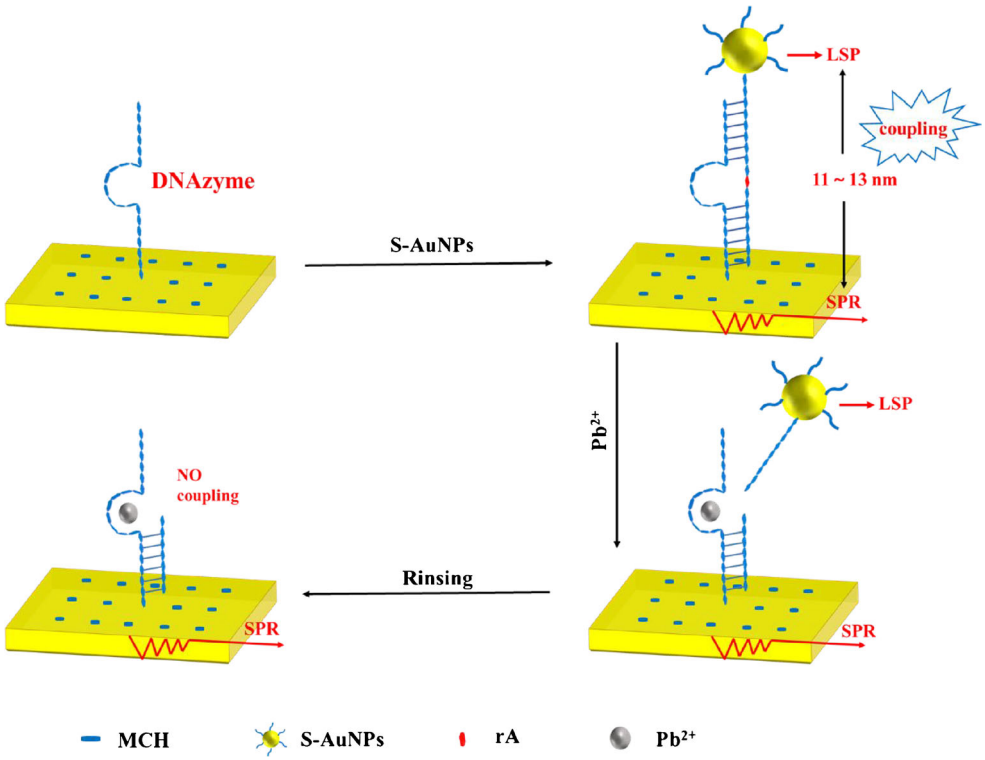

Fig. 1 Detection strategy of the Pb^{2+} sensor based on DNAzyme and SPR with LSP-SPP coupling

published results for self-assembled thiol-modified DNA monolayers on gold surface [42, 43].

According to the stoichiometry for DNAzyme (C367 N134 O261 P37 S1) and MCH (C6 O1 S1), the atomic ratios of C/O were used to estimate the molecular percentage of DNAzyme and MCH (Table 1). Carbon and oxygen were selected for the estimation because of the high signal-to-noise ratio of their XPS spectra, regardless of the negligible adventitious hydrocarbons on the DNA films. To determine the coverage of DNAzyme and MCH, sulfur was used as the reference signal and the S 2p/Au 4f intensity ratio was calculated. The obtained ratio of $(6.4 \pm 1.2) \times 10^{-3}$ agrees well with the theoretical (0.0061) and measured (0.0063) intensity ratios of S 2p/Au 4f for the saturation coverage of octanethiol on gold [44, 45]. Given the molecular percentage of DNAzyme in Table 1 and the saturated S coverage of 4.6×10^{14} atoms/cm^2 on gold surface reported by Kawasaki's work [44], the DNAzyme coverage was simply obtained from the product of them. The coverage values in Table 1 are comparable with the reported DNA coverage (5.2×10^{12}–7.6×10^{12} molecules/cm^2) of similar MCH-treated monolayer of thiol-modified single-strand DNA on a gold surface. As expected, the DNAzyme coverage on the SPR chip surface increases with the concentration of DNAzyme solution. These results demonstrate that the surface coverage of DNAzyme has been tailored using MCH and different DNAzyme concentrations. Controlling the surface coverage of DNAzyme would contribute to optimizing that of AuNPs through DNAzyme-substrate hybridization and consequently the sensitivity of SPR sensors.

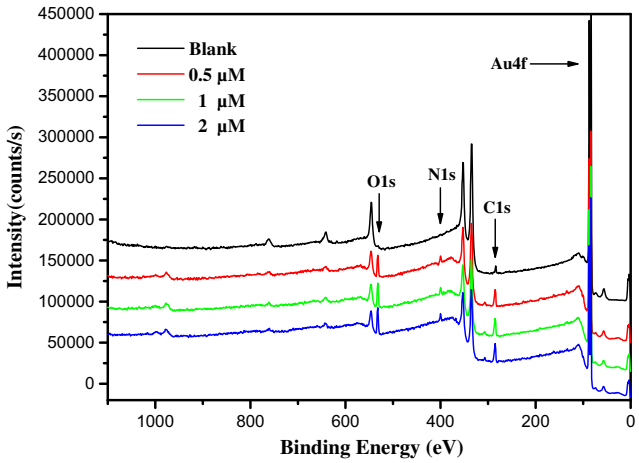

Fig. 2 XPS spectra of sensor chips modified with DNAzyme of various concentrations

Table 1 Surface coverage of DNAzyme based on elemental and molecular ratios on sensor chips prepared with different concentrations of DNAzyme solutions

Concentration (μM)	C/O	DNAzyme percentage (%)	DNAzyme coverage ($\times 10^{12}$ DNA/cm^2)
0.5	2.339	1.482	6.8
1.0	2.281	1.603	7.4
2.0	2.144	1.964	9.0

Immobilization of S-AuNPs through the hybridization of DNAzyme with the substrate is essential for sensor fabrication. Surfaces of the fabricated sensor chips before and after Pb^{2+} detection were characterized by SEM for comparison (Fig. 3). As compared with the bare sensor surface (ESM Fig. S3a), a large number of AuNPs covered the sensor chip surface after the sensor fabrication (Fig. 3a). AuNPs evenly distributed on the surface of the SPR sensor chip, indicating limited aggregation of AuNPs. The SEM image demonstrates the successful immobilization of DNAzyme-S-AuNP conjugates on the sensor chip. The coverage of AuNPs is estimated to be 6.7×10^{10} particles/cm^2 by counting the particles in the SEM image. This coverage is sufficient to achieve a high sensitivity of SPR sensors [36].

In the presence of Pb^{2+}, the removal of AuNPs from the sensor surface due to the cleavage of the substrate strand was monitored by SPR reflectivity curves. Each of the SPR curves features a typical "SPR dip" with a reflectivity minimum at the SPR angle (Fig. 4). The SPR angles for 10–1000 nM Pb^{2+} shift negatively associated with recovery in reflectivity compared with that for the blank sample. The negative shift of the SPR angle was because of the decrease in the refractive index of the sensing layer due to the removal of S-AuNP. Since the amount of cleaved substrate depends on the concentration of Pb^{2+}, the SPR angle changes with the concentration of Pb^{2+}, which confirms the proposed sensing principle. In order to verify the change of the SPR response signal, the SEM image was obtained for the SPR chip surface reacted with 1000 nM of Pb^{2+} (Fig. 3b). The number of AuNPs on the SPR chip surface reduced significantly, resulting in the coverage of 2.6×10^{10} particles/cm^2. The reduced amount of AuNPs led to a shift in the SPR response signal due to a quasi-linear relationship between AuNP coverage and SPR angle shift [36]. In contrast, the blank sample did not alter the surface coverage of AuNPs (ESM Fig. S3b).

Sensor capability of Pb^{2+} detection

In order to study the performance of the fabricated SPR sensor, the SPR sensors were incubated with Pb^{2+} solutions of different concentrations, and the changes of the SPR response signal were monitored online. The incubation time was optimized and set to 25 min for the substrate cleavage reaction to reach equilibrium, and the shift in SPR angle was recorded. Figure 5 shows the changes in SPR angle against the concentration of Pb^{2+} for the three groups of sensors modified with DNAzyme concentration of 0.5, 1, and 2 μM. As the Pb^{2+} concentration increased from 10 to 1000 nM, the change in SPR angle gradually increased and reached the saturation of the cleaving reaction sites at the rA position on the substrate. For each group of sensors, a linear relationship ($R^2 > 0.95$) between the SPR angle changes and the logarithm of Pb^{2+} concentrations was observed before the SPR response reached saturation. The slope of the linear fit and the standard deviation (σ) of blank measurements are shown in Table S1 (see ESM). Based on 3σ/slope, the detection limits of the three SPR sensors were 209 pM, 80 pM, and 198 pM for DNAzyme concentration of 0.5, 1, and 2 μM, respectively. The detection limits are two or three orders of magnitude lower than the toxicity levels of Pb^{2+} in drinking water defined by WHO and USEPA. The dynamic range was up to 1000 nM, 100 nM, and 2000 nM for 0.5, 1, and 2 μM DNAzyme, respectively. At least four orders of magnitude in Pb^{2+} concentration were covered by all of the three sensors.

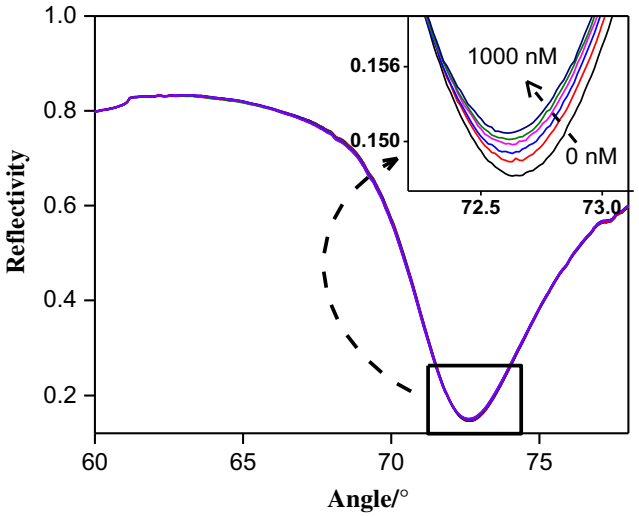

Fig. 4 SPR angular reflectivity curves corresponding to the detection of Pb^{2+} with different concentrations (only 0, 10, 50, 100, 500, and 1000 nM are shown for clarity)

The high sensitivity of the reported SPR sensors is attributed to the AuNPs bound to the sensor surface through the DNAzyme-substrate linkage. Signal amplification is partly

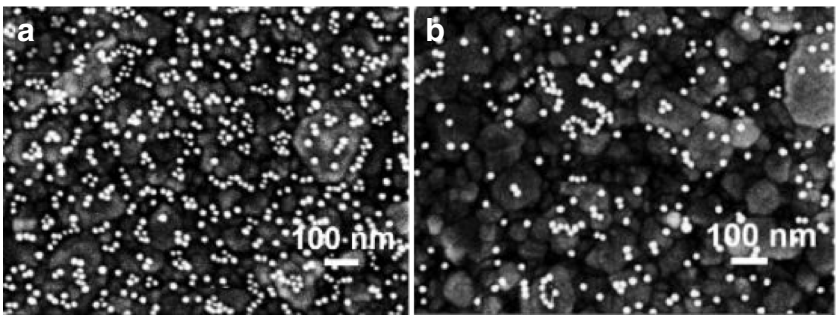

Fig. 3 SEM topographic images of fabricated sensor chips **a** before and **b** after detection of 1000 nM Pb^{2+}

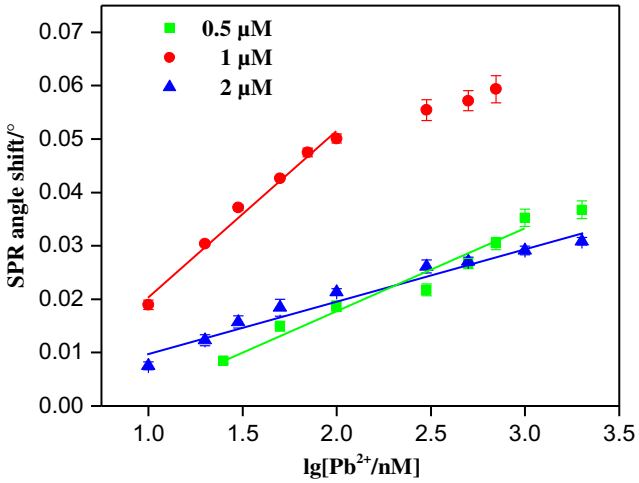

Fig. 5 Responses of SPR sensors fabricated with 0.5, 1, and 2 μM DNAzyme for Pb^{2+} detection. Error bars are standard deviations of three repetitive experiments

due to the additional mass of AuNPs and an increase in the refractive index near the sensor surface [46]. Moreover, the plasmonic coupling between the LSP of AuNPs and the SPP on the gold chip surface plays a more important role in inducing a greater SPR incident angle shift. This effect has been verified by studies comparing AuNPs with non-resonant particles such as latex particles. The findings imply that the increase in bound mass is not the only factor resulting in SPR signal amplification [47]. The LSP-SPP coupling is very strong when the distance between AuNPs and the gold surface is within ~ 50 nm [48]. Since the length of hybridized DNAzyme-substrate is within 20 nm, the AuNPs with LSP (evidenced by ESM Fig. S1) are in the range of coupling with the SPP. Therefore, the LSP-SPP coupling could be expected to occur. The effects of coupling on SPR signals depend on multiple factors including the size, shape, and surface coverage of AuNPs as well as AuNP-surface distance, and wavelength of the laser used in SPR sensors [48–50]. For instance, gold nanorod demonstrates more intensive LSP-SPP coupling [40].

The dependence of the sensitivity on the DNAzyme concentration is consistent with the similar sensing method using QCM-D [30]. The sensitivity and dynamic range of sensors are always influenced by the surface density of recognition elements [51]. For 0.5 μM DNAzyme, the surface density of DNAzyme and consequently the DNAzyme-S-AuNP conjugates on the sensor surface may be insufficient, so the SPR shift due to AuNP removal was insignificant. With the surface density of DNAzyme increased to 1 μM, the SPR signal was enhanced by the increased amount of DNAzyme-S-AuNP conjugates, but it tended to saturate for high Pb^{2+} concentrations due to the consumption of DNAzyme-S-AuNP conjugates. When the density of DNAzyme was so high as 2 μM, binding of S-AuNPs might have been blocked by the steric hindrance effect [52, 53]. Moreover, one 15-nm AuNP could be capped by numerous thiol-functionalized oligonucleotides [54]. Given the much higher surface density of DNAzyme compared with that of AuNPs, one AuNP could bind to the sensor surface through multiple DNAzyme-substrate structures, implying that the DNAzyme concentration would also determine the strength of AuNP binding on the sensor surface. Excessive DNAzyme-substrate bindings would require high-concentration Pb^{2+} ions for efficient removal of AuNPs, so the sensor sensitivity was lowered by the high DNAzyme concentration, and the Pb^{2+} capacity of the sensor was enlarged as shown by the widened dynamic range. Therefore, an optimal DNAzyme concentration is essential for maintaining the appropriate surface density of DNAzyme-S-AuNP conjugates, and the sensor performance is controllable by tuning the coverage of DNAzyme.

It is challenging to fulfill the requirements of easy to use and high sensitivity in one heavy metal ion sensor. Previous studies on label-free, DNAzyme-based Pb^{2+} detection in water reported a detection limit of 14 nM with AuNP-enhanced QCM-D [30], 1.0 nM with silver nanoparticle–modified SERS [55], and 0.25 nM and 46 pM with the ferrocene-functionalized electrochemical sensors [56, 57]. Label-free SPR sensors were also reported with detection limits ranging from sub-micromolar to 0.01 nM using composites of graphene oxide [35, 58]. Sensors with even higher sensitivities have also been reported [59–61]. However, most of these methods have undergone time-consuming and multi-step secondary signal amplification during or after the reaction with sample solutions. Onsite labeling and processing of DNA-containing solutions may also introduce experimental error to the sensors. A summary of detection modes, detection limits, and dynamic ranges of more previous studies is given in Table S2 (see ESM). Our method can directly detect Pb^{2+} with high sensitivity using sensor chips fabricated in advance. While sensitivities of our sensors are not as high as the methods incorporating active labels using electrochemical and SERS techniques, the benefits of this label-free and direct detection method should be highlighted. Meanwhile, the detection performance of commercial portable SPR devices [33] is comparable with that of the current instrument used without reference channel correction. Given the quick progress in the miniaturization of SPR sensors [34, 62], it would be feasible to utilize this method for the development of portable Pb^{2+} sensing devices. Moreover, the sensitivities of our SPR sensors could be further improved by tuning the near-field coupling effects [63]. For example, the use of gold nanostars and nanocubes has achieved attomolar detection by SPR [64, 65]. The LSP-SPP interactions would also become more significant at incident wavelengths close to the LSP resonance of the AuNPs [66].

Selectivity and real sample analysis

By detecting several higher concentration (1000 nM) divalent metal ions (Co^{2+}, Cd^{2+}, Cu^{2+}, Fe^{2+}, Ni^{2+}, and

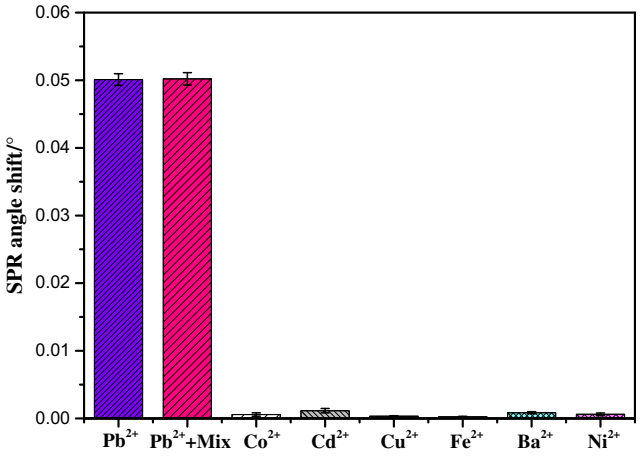

Fig. 6 Selectivity of the SPR biosensor in detection of 100 nM Pb^{2+}, 1000 nM interferencing metal ions, and a mixture of them

Ba^{2+}), the selectivity of this sensor for Pb^{2+} was studied using the optimized sensor fabricated with 1 μM DNAzyme. As shown in Fig. 6, the SPR response of other metal ions changed very little, even though their concentrations were 10 times higher than that of Pb^{2+} (100 nM). Moreover, the disturbing ions did not influence the SPR response when mixed with Pb^{2+}. The results prove the negligible interference of these metal ions on the DNAzyme-based SPR sensor. This demonstrates the excellent selectivity of this method for Pb^{2+}.

To evaluate the practical performance of the SPR sensor for detecting Pb^{2+}, groundwater samples from Bao'an District of Shenzhen City were analyzed. After passing through a 0.45-μm filter membrane, the groundwater was spiked with 25, 50, and 100 nM Pb^{2+} solutions, respectively. Freshly fabricated SPR sensors were used to detect Pb^{2+} in the solutions. As shown in Table 2, the recovery rate of this method is between 96.8 and 108.5%. Meanwhile, the analysis of Pb^{2+} in the same solutions by ICP-MS showed that the data had satisfactory accuracy and consistency. These results indicate that the SPR sensors reported in this work have a reliable performance for detecting real samples.

Table 2 Determination of Pb^{2+} concentration in groundwater samples

Added (nM)	Measured (nM, mean[a] ± SD[b])	Recovery (%)	ICP-MS (nM, mean[a] ± SD[b])
0	0	/	0.002 ± 0.001
25	24.2 ± 0.10	96.8	24.83 ± 0.07
50	51.8 ± 0.28	103.6	50.60 ± 0.15
100	108.5 ± 1.09	108.5	100.72 ± 0.20

[a] Mean: average value of three individual experiments

[b] SD: standard deviation of three individual experiments

Conclusions

In summary, we have developed a sensitive, selective, and easy-to-use DNAzyme-based SPR sensor for the detection of Pb^{2+} ions in water. This method benefits from the label-free nature of the SPR technique and its highly intense coupling with LSP of AuNPs. The detection limit is 80 pM for the optimal sensor without the need for sample labeling or secondary signal amplification. The sensitivity and dynamic range of the sensors are controllable by tuning the surface density of DNAzyme. The sensor is also extremely selective for Pb^{2+} compared with other metal ions. The satisfactory results of groundwater analysis provide this method with the possibility of practical applications. Compared with conventional technologies, this method has more potential for developing cost-effective and miniaturized devices, enabling the onsite and rapid detection of Pb^{2+} ion in water. The sensitivity of this method would be further improved by tuning the shape and surface coverage of AuNPs as well as optimizing SPR incident wavelength. Moreover, given the diversity of metal-specific DNAzymes, the detection strategy is also versatile for detecting a wide range of metal ions.

Funding information This research was supported by the National Key R&D Program of China (2018YFC1902903) and Shenzhen Science and Technology Innovation Committee (JSGG20170822164024506 and KJYY20171012103638606).

Compliance with ethical standards

Conflict of interest The authors declare that they have no conflict of interest.

References

1. Yang QQ, Li ZY, Lu XN, Duan QN, Huang L, Bi J. A review of soil heavy metal pollution from industrial and agricultural regions in China: pollution and risk assessment. Sci Total Environ. 2018;642:690–700.
2. Khoshbin Z, Housaindokht MR, Verdian A, Bozorgmehr MR. Simultaneous detection and determination of mercury (II) and lead (II) ions through the achievement of novel functional nucleic acid-based biosensors. Biosens Bioelectron. 2018;116:130–47.
3. Babu SH, Kumar KS, Suvardhan K, Kiran K, Rekha D, Krishnaiah L, et al. Preconcentration technique for the determination of trace elements in natural water samples by ICP-AES. Environ Monit Assess. 2007;128(1–3):241–9.
4. Cocherie A, Robert M. Direct measurement of lead isotope ratios in low concentration environmental samples by MC-ICP-MS and multi-ion counting. Chem Geol. 2007;243(1–2):90–104.
5. Mortada WI, Kenawy IMM, Abdelghany AM, Ismal AM, Donia AF, Nabieh KA. Determination of Cu2+ Zn2+ and Pb2+ in biological and food samples by FAAS after preconcentration with hydroxyapatite nanorods originated from eggshell. Mater Sci Eng C. 2015;52:288–96.
6. Liu S, Sun JS, Huo JZ, Duan XC, Liu Y. Room-temperature chelate vapor generation of lead using ammonium O,O-diethyl

dithiophosphate as a chelating reagent and determination by atomic fluorescence spectrometry in environmental water samples. Anal Sci. 2019;35(5):499–504.
7. Sun Q, Wang J, Tang M, Huang L, Zhang Z, Liu C, et al. A new electrochemical system based on a flow-field shaped solid electrode and 3D-printed thin-layer flow cell: detection of Pb2+ ions by continuous flow accumulation square-wave anodic stripping voltammetry. Anal Chem. 2017;89(9):5024–9.
8. Malik LA, Bashir A, Qureashi A, Pandith AH. Detection and removal of heavy metal ions: a review. Environ Chem Lett. 2019;17(4):1495–521.
9. Zhao G, Liu G. A portable electrochemical system for the on-site detection of heavy metals in farmland soil based on electrochemical sensors. IEEE Sensors J. 2018;18(14):5645–55.
10. Lu W, Lin C, Yang J, Wang X, Yao B, Wang M. A DNAzyme assay coupled with effective magnetic separation and rolling circle amplification for detection of lead cations with a smartphone camera. Anal Bioanal Chem. 2019;411(21):5383–91.
11. Kim H, Jang G, Yoon Y. Specific heavy metal/metalloid sensors: current state and perspectives. Appl Microbiol Biotechnol. 2020;104(3):907–14.
12. Liang G, Man Y, Li A, Jin X, Liu X, Pan L. DNAzyme-based biosensor for detection of lead ion: a review. Microchem J. 2017;131:145–53.
13. Cuenoud B, Szostak JW. A DNA metalloenzyme with DNA-ligase activity. Nature. 1995;375(6532):611–4.
14. Tan Y, Qiu J, Cui M, Wei X, Zhao M, Qiu B, et al. An immobilization free DNAzyme based electrochemical biosensor for lead determination. Analyst. 2016;141(3):1121–6.
15. Liang H, Xie S, Cui L, Wu C, Zhang X. Designing a biostable L-DNAzyme for lead(II) ion detection in practical samples. Anal Methods. 2016;8(39):7260–4.
16. Cheng Y, Huang Y, Lei J, Zhang L, Ju H. Design and biosensing of Mg2+-dependent DNAzyme-triggered ratiometric electrochemiluminescence. Anal Chem. 2014;86(10):5158–63.
17. Zhou Y, Tang L, Zeng G, Zhang C, Zhang Y, Xie X. Current progress in biosensors for heavy metal ions based on DNAzymes/DNA molecules functionalized nanostructures: a review. Sens Actuators B Chem. 2016;223:280–94.
18. Lan T, Furuya K, Lu Y. A highly selective lead sensor based on a classic lead DNAzyme. Chem Commun. 2010;46(22):3896–8.
19. Lee JH, Wang Z, Liu J, Lu Y. Highly sensitive and selective colorimetric sensors for uranyl (UO22+): development and comparison of labeled and label-free DNAzyme-gold nanoparticle systems. J Am Chem Soc. 2008;130(43):14217–26.
20. Brown AK, Liu J, He Y, Lu Y. Biochemical characterization of a uranyl ion-specific DNAzyme. Chembiochem. 2009;10(3):486–92.
21. Fu T, Ren S, Gong L, Meng H, Cui L, Kong R-M, et al. A label-free DNAzyme fluorescence biosensor for amplified detection of Pb2+-based on cleavage-induced G-quadruplex formation. Talanta. 2016;147:302–6.
22. Liu MY, Lou XH, Du J, Guan M, Wang J, Ding XF, et al. DNAzyme-based fluorescent microarray for highly selective and sensitive detection of lead (II). Analyst. 2012;137(1):70–2.
23. Wang H-B, Wang L, Huang K-J, Xu S-P, Wang H-Q, Wang L-L, et al. A highly sensitive and selective biosensing strategy for the detection of Pb2+ ions based on GR-5 DNAzyme functionalized AuNPs. New J Chem. 2013;37(8):2557–63.
24. Yun W, Cai D, Jiang J, Zhao P, Huang Y, Sang G. Enzyme-free and label-free ultra-sensitive colorimetric detection of Pb2+ using molecular beacon and DNAzyme based amplification strategy. Biosens Bioelectron. 2016;80:187–93.
25. Yang X, Xu J, Tang X, Liu H, Tian D. A novel electrochemical DNAzyme sensor for the amplified detection of Pb2+ ions. Chem Commun. 2010;46(18):3107–9.
26. Xiao Y, Rowe AA, Plaxco KW. Electrochemical detection of parts-per-billion lead via an electrode-bound DNAzyme assembly. J Am Chem Soc. 2007;129(2):262–3.
27. Ji R, Niu W, Chen S, Xu W, Ji X, Yuan L, et al. Target-inspired Pb2+−dependent DNAzyme for ultrasensitive electrochemical sensor based on MoS2-AuPt nanocomposites and hemin/G-quadruplex DNAzyme as signal amplifier. Biosens Bioelectron. 2019;144:111560.
28. Tian A, Liu Y, Gao J. Sensitive SERS detection of lead ions via DNAzyme based quadratic signal amplification. Talanta. 2017;171:185–9.
29. Wang Y, Irudayaraj J. A SERS DNAzyme biosensor for lead ion detection. Chem Commun. 2011;47(15):4394–6.
30. Teh HB, Li H, Li SFY. Highly sensitive and selective detection of Pb2+ ions using a novel and simple DNAzyme-based quartz crystal microbalance with dissipation biosensor. Analyst. 2014;139(20):5170–5.
31. Daniya WMEMM, Saleviter S, Fen YW. Development of surface plasmon resonance spectroscopy for metal ion detection. Sens Mater. 2018;30(9):2023–38.
32. Fen YW, Yunus WMM. Surface plasmon resonance spectroscopy as an alternative for sensing heavy metal ions: a review. Sens Rev. 2013;33(4):305–14.
33. Wu H, Li H, Chua FZH, Li SFY. Rapid detection of melamine based on immunoassay using portable surface plasmon resonance biosensor. Sens Actuators B Chem. 2013;178:541–6.
34. Guner H, Ozgur E, Kokturk G, Celik M, Esen E, Topal AE, et al. A smartphone based surface plasmon resonance imaging (SPRi) platform for on-site biodetection. Sens Actuators B Chem. 2017;239:571–7.
35. Alwahib AAA, Kamil YM, Abu Bakar MH, Noor ASM, Yaacob MH, Lim HN, et al. Reduced graphene oxide/maghemite nanocomposite for detection of lead ions in water using surface plasmon resonance. IEEE Photon J. 2018;10(6):1–10.
36. Lyon LA, Musick MD, Natan MJ. Colloidal Au-enhanced surface plasmon resonance immunosensing. Anal Chem. 1998;70(24):5177–83.
37. Zeng S, Yong K-T, Roy I, Dinh X-Q, Yu X, Luan F. A review on functionalized gold nanoparticles for biosensing applications. Plasmonics. 2011;6(3):491–506.
38. Fathi F, Rashidi M-R, Omidi Y. Ultra-sensitive detection by metal nanoparticles-mediated enhanced SPR biosensors. Talanta. 2019;192:118–27.
39. Wang L, Li T, Du Y, Chen C, Li L, Zhou M, et al. Au NPs-enhanced surface plasmon resonance for sensitive detection of mercury (II) ions. Biosens Bioelectron. 2010;25(12):2622–6.
40. Mustafa DE, Yang T, Xuan Z, Chen S, Tu H, Zhang A. Surface plasmon coupling effect of gold nanoparticles with different shape and size on conventional surface plasmon resonance signal. Plasmonics. 2010;5(3):221–31.
41. Guo L, Jackman JA, Yang H-H, Chen P, Cho N-J, Kim D-H. Strategies for enhancing the sensitivity of plasmonic nanosensors. Nano Today. 2015;10(2):213–39.
42. Petrovykh DY, Kimura-Suda H, Whitman LJ, Tarlov MJ. Quantitative analysis and characterization of DNA immobilized on gold. J Am Chem Soc. 2003;125(17):5219–26.
43. Jia Y, Li F. Studies of functional nucleic acids modified light addressable potentiometric sensors: X-ray photoelectron spectroscopy, biochemical assay, and simulation. Anal Chem. 2018;90(8):5153–61.
44. Kawasaki M, Sato T, Tanaka T, Takao K. Rapid self-assembly of alkanethiol monolayers on sputter-grown Au(111). Langmuir. 2000;16(4):1719–28.
45. Petrovykh DY, Kimura-Suda H, Tarlov MJ, Whitman LJ. Quantitative characterization of DNA films by X-ray photoelectron spectroscopy. Langmuir. 2004;20(2):429–40.

46. He L, Musick MD, Nicewarner SR, Salinas FG, Benkovic SJ, Natan MJ, et al. Colloidal Au-enhanced surface plasmon resonance for ultrasensitive detection of DNA hybridization. J Am Chem Soc. 2000;122(38):9071–7.
47. Besselink GAJ, Kooyman RPH, van Os P, Engbers GHM, Schasfoort RBM. Signal amplification on planar and gel-type sensor surfaces in surface plasmon resonance-based detection of prostate-specific antigen. Anal Biochem. 2004;333(1):165–73.
48. Mock JJ, Hill RT, Degiron A, Zauscher S, Chilkoti A, Smith DR. Distance-dependent plasmon resonant coupling between a gold nanoparticle and gold film. Nano Lett. 2008;8(8):2245–52.
49. Frasconi M, Tortolini C, Botre F, Mazzei F. Multifunctional au nanoparticle dendrimer-based surface plasmon resonance biosensor and its application for improved insulin detection. Anal Chem. 2010;82(17):7335–42.
50. Hinman SS, McKeating KS, Cheng Q. Surface plasmon resonance: material and interface design for universal accessibility. Anal Chem. 2018;90(1):19–39.
51. Qiu G, Ng SP, Liang X, Ding N, Chen X, Wu C-ML. Label-free LSPR detection of trace lead(II) ions in drinking water by synthetic poly(mPD-co-ASA) nanoparticles on gold nanoislands. Anal Chem. 2017;89(3):1985–93.
52. Wang JJ, Morabito K, Tang JX, Tripathi A. Microfluidic platform for isolating nucleic acid targets using sequence specific hybridization. Biomicrofluidics. 2013;7:044107.
53. Jiang KR, Huang JL, Chen CC, Su HJ, Wu JC. Effect of co-axially hybridized gene targets on hybridization efficiency of microarrayed DNA probes. J Taiwan Inst Chem Eng. 2011;42(1):5–12.
54. Demers LM, Mirkin CA, Mucic RC, Reynolds RA, Letsinger RL, Elghanian R, et al. A fluorescence-based method for determining the surface coverage and hybridization efficiency of thiol-capped oligonucleotides bound to gold thin films and nanoparticles. Anal Chem. 2000;72(22):5535–41.
55. Fu C, Xu W, Wang H, Ding H, Liang L, Cong M, et al. DNAzyme-based plasmonic nanomachine for ultrasensitive selective surface-enhanced Raman scattering detection of lead ions via a particle-on-a-film hot spot construction. Anal Chem. 2014;86(23):11494–7.
56. Zhang Y, Xiao S, Li H, Liu H, Pang P, Wang H, et al. A Pb2+-ion electrochemical biosensor based on single-stranded DNAzyme catalytic beacon. Sens Actuators B Chem. 2016;222:1083–9.
57. Ma R-N, Wang LL, Zhang M, Jia L-P, Zhang W, Shang L, et al. A novel one-step triggered "signal-on/off" electrochemical sensing platform for lead based on the dual-signal ratiometric output and electrode-bound DNAzyme assembly. Sens Actuators B Chem. 2018;257:678–84.
58. Fen YW, Yunus WMM, Yusof NA. Surface plasmon resonance optical sensor for detection of Pb2+ based on immobilized p-tert-butylcalix 4 arene-tetrakis in chitosan thin film as an active layer. Sens Actuators B Chem. 2012;171:287–93.
59. Liao X, Luo J, Wu J, Fan T, Yao Y, Gao F, et al. A sensitive DNAzyme-based electrochemical sensor for Pb2+ detection with platinum nanoparticles decorated TiO2/alpha-Fe2O3 nanocomposite as signal labels. J Electroanal Chem. 2018;829:129–37.
60. Wu J, Wei S, Lu Y, Ren N, Bian X, Zhang J. Ultrasensitive DNAzyme-based electrochemical biosensor for Pb2+ based on FcHT-mediated biocatalytic amplification. Int J Electrochem Sci. 2018;13(10):9630–41.
61. Yu Z, Li N, Hu X, Dong Y, Lin Y, Cai H, et al. Highly efficient electrochemical detection of lead ion using metal-organic framework and graphene as platform based on DNAzyme. Synth Met. 2019;254:164–71.
62. Jing JY, Zhu Q, Dai ZX, Li SY, Wang Q, Zhao WM. Sensing self-referenced fiber optic long-range surface plasmon resonance sensor based on electronic coupling between surface plasmon polaritons. Appl Opt. 2019;58(23):6329–34.
63. Shalabney A, Abdulhalim I. Sensitivity-enhancement methods for surface plasmon sensors. Laser Photonics Rev. 2011;5(4):571–606.
64. Kim S, Lee HJ. Gold nanostar enhanced surface plasmon resonance detection of an antibiotic at attomolar concentrations via an aptamer-antibody sandwich assay. Anal Chem. 2017;89(12):6624–30.
65. Jang HR, Wark AW, Baek SH, Chung BH, Lee HJ. Ultrasensitive and ultrawide range detection of a cardiac biomarker on a surface plasmon resonance platform. Anal Chem. 2014;86(1):814–9.
66. Hutter E, Fendler JH, Roy D. Surface plasmon resonance studies of gold and silver nanoparticles linked to gold and silver substrates by 2-aminoethanethiol and 1,6-hexanedithiol. J Phys Chem B. 2001;105(45):11159–68.